

# Unveiling the Role of Key Parameters during Molecular Growth for Optimal Poly(glycerol sebacate) Synthesis

Rubén Martín-Cabezuelo,\* Alicia Naderpour-Peñalver, A Sigen, Wenxin Wang, Guillermo Vilariño-Feltrer, and Ana Vallés-Lluch

Poly(glycerol sebacate) (PGS) belongs to the hyperbranched polyesters family (HBP), which possesses an extensive variety of applications due to its tunable chemical and mechanical properties, together with its biocompatibility and biodegradability. However, the understanding of PGS synthesis becomes a challenge due to the lack of consistency when determining its synthesis parameters. Understanding these parameters is fundamental to control PGS synthesis and obtain a scalable and reproducible final product for biomedical applications. To unveil their effect on diverging PGS properties, diols are used as glycerol analogs and the reaction is chemically and thermally monitored, suggesting a heterogeneous reactivity of the exposed hydroxyl groups. Also, confinement of the prepolymerization is proven to be fundamental. In order to maintain the equimolar ratio of initial monomers during synthesis, early stages of the polycondensation (first 4 h) tend to linear and less branched oligomers by consuming primary hydroxyls rather than secondary hydroxyls. However, physicochemical characterization determines that a high degree of conversion (40%) is reached during these early stages. Afterward, the oligomers tend to condense through the secondary hydroxyls into a more crosslinked elastomer. This study demonstrates how hydroxyl affinity, water presence, and glycerol loss are crucial for the scalability and reproducibility of its final product.

## 1. Introduction

Hyperbranched polyesters (HBP), studied for the first time by Young H. Kim and Owen W. Webster in the early 1990s,<sup>[1]</sup> are random branch-on-branch topology dendritic macromolecules.<sup>[1]</sup> HBP characteristics, such as controlled molecular weight, wide range of polydispersity, and high degree of branching,<sup>[2,3]</sup> enable their applications in several fields, including drug delivery, biosensing and imaging, catalysis or nanoencapsulation, among others.<sup>[3–13]</sup>

Particularly, poly(glycerol sebacate) (PGS) is one of the most studied HBP thus far.<sup>[14–17]</sup> This is because, in addition to common HBP characteristics, PGS shows polyvalent properties for biomedical and tissue engineering (TE) applications. PGS monomers are glycerol (Gly) and sebacic acid (SA), both approved by the FDA.<sup>[18,19]</sup> The most distinct PGS properties are biodegradability and biocompatibility. Conventionally, PGS synthesis begins with a 24 h prepolymerization of an equimolar ratio of its reagents, Gly and SA, under inert atmosphere flow, followed by 24 to

48 h curing in an oven, both steps carried out at 130 °C.<sup>[20–22]</sup> After prepolymerization, the formation of still soluble branched oligomeric and/or macromeric structures occurs, by means of the polycondensation of primary hydroxyls (pOH) from Gly with the carboxyl groups of SA. Afterward, the prepolymer reaction continues in the solid phase during polymerization, where the crosslinking of the network forms.<sup>[2,23,24]</sup>


Nevertheless, several studies have shown how the wide variability within PGS production leads to diverging end properties.<sup>[15,20,25–30]</sup> This fact emphasizes the need to fully understand the role of PGS synthesis parameters, assumedly based on typical HBP formation via a two-step polycondensation system.

Thus, the aim of this study is to shed light on PGS synthesis parameters: the effect of Gly hydroxyl functionality and the understanding of the kinetics of polycondensation reaction, degree of branching, and the loss of Gly and water during the reaction. The latter factor may play a key role during early stages of PGS synthesis, and it has been overlooked on mainstream PGS synthesis protocols.<sup>[15]</sup> For that purpose, different synthesis scenarios were evaluated, using similar Gly alcohols

R. Martín-Cabezuelo, A. Naderpour-Peñalver, G. Vilariño-Feltrer, A. Vallés-Lluch  
Centre for Biomaterials and Tissue Engineering  
Technical University of Valencia  
Valencia 46020, Spain  
E-mail: rubmarca@doctor.upv.es

A Sigen, W. Wang  
Charles Institute of Dermatology  
School of Medicine  
University College Dublin  
Dublin D04 V1W8, Ireland

A. Vallés-Lluch  
Biomedical Research Networking Centre in Bioengineering  
Biomaterials and Nanomedicine (CIBER-BBN)  
Valencia Spain

 The ORCID identification number(s) for the author(s) of this article can be found under <https://doi.org/10.1002/mame.202300270>

© 2023 The Authors. Macromolecular Materials and Engineering published by Wiley-VCH GmbH. This is an open access article under the terms of the Creative Commons Attribution License, which permits use, distribution and reproduction in any medium, provided the original work is properly cited.

DOI: 10.1002/mame.202300270

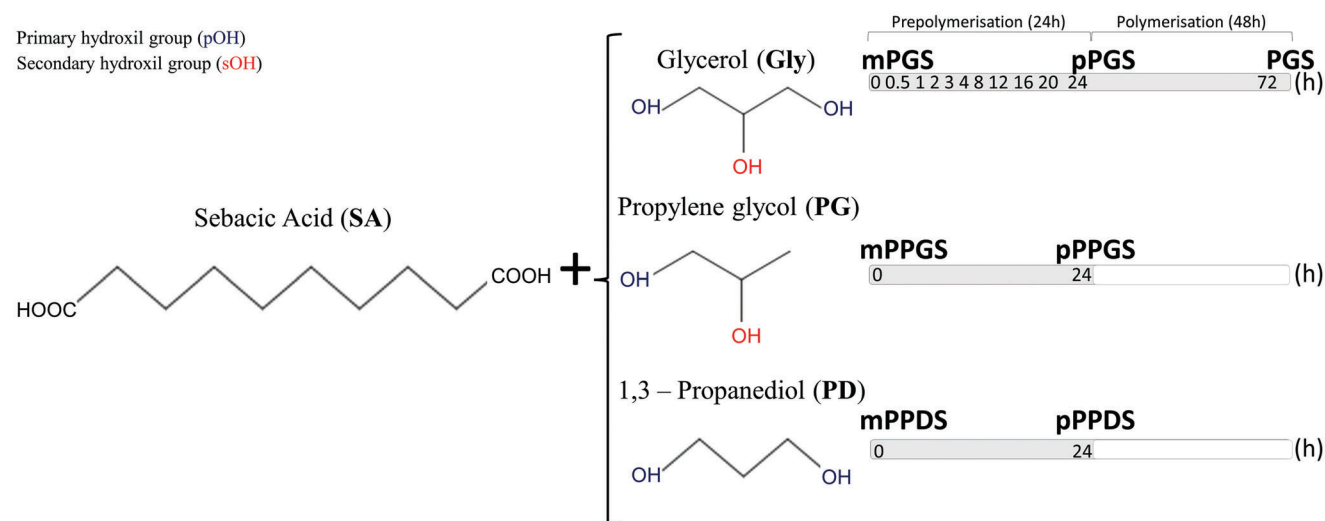


**Figure 1.** Schematic representation of the synthesis of different polyols polyesters.

and different environmental conditions to understand PGS key synthesis steps (Figure 1). Gly chemical structure possesses two primary (pOH) and one secondary (sOH) hydroxyl groups. While pOH groups provide the linear component of the PGS backbone, sOH are the ones directly related to the crosslink and network formation of the PGS. Furthermore, sOH groups are usually less reactive than the primary groups.<sup>[24,31]</sup>

PGS polycondensation reaction was monitored by titration, FTIR and <sup>1</sup>H-NMR spectroscopy over reaction time. Previous works have studied glycerol-based hyperbranched polymers using nuclear magnetic resonance techniques and validated the chemical shift assignments, demonstrating that the technique is sensitive enough to determine the glycerol and its 5 possible derivatives resulting from its polycondensation with SA.<sup>[24,32–34]</sup> Complementary characterization techniques such as differential scanning calorimetry and thermogravimetric analysis were also used.

## 2. Experimental Section

### 2.1. Prepolymerization of Poly(glycerol sebacate) and Alternatives

Equimolar (1:1) or stoichiometric (3:2) ratios of Gly (>99.5%, Sigma Aldrich) and SA (>99%, Sigma Aldrich) were mixed under N<sub>2</sub> flow in a round bottom flask at 130 °C. The starting point of the prepolymerization reaction (t = 0 h) was set once the mixture of monomers (mPGS) was melted homogeneously. As the prepolymerisation progressed (0 h < t < 24 h), samples of PGS prepolymer (pPGS) were collected at different time points and left to cool down to room temperature.

Similar mixtures were prepared with 1,3-propanediol (PD, Sigma Aldrich) and propylene glycol (PG, >99.5%, Sigma Aldrich) instead of Gly, at equimolar and stoichiometric ratios with SA, leading to PPDS and PPGS, respectively. Samples were collected at t = 0 h (monomer mixtures mPPDS and mPPGS) and t = 24 h (prepolymers pPPDS and pPPGS).

### 2.2. Curing of Poly(glycerol sebacate)

The resulting pPGS obtained from prepolymerization of mPGS was collected after 24 h of reaction and cured in open square molds made of Teflon® at 130 °C in a forced ventilation oven for 48 h, to obtain 1 mm-thick PGS films.

To remove unreacted monomer residues and uncrosslinked chains, PGS films were washed in tetrahydrofuran (THF ≥99.0%, Scharlau) for two days on an orbital shaker. THF was progressively replaced with ethanol (EtOH >99%, Scharlau). Last, EtOH was gradually replaced with ultrapure MilliQ water over the last two days. To conclude, PGS films were dried under vacuum conditions for 24 h.

### 2.3. Characterization of poly(glycerol sebacates) Based on Alcohols with Different Functionalities

#### 2.3.1. Rheology Measurements

To track the viscosity of poly(glycerol sebacate) samples during prepolymerization, gelation and curing, a Discovery HR-2 hybrid rheometer (TA Instruments, Waters™, USA) was used. Monomer mixtures were placed between disposable 25 mm-diameter parallel aluminum plates, separated by a gap of 1000 μm. Viscosity was monitored every 300 s throughout the curing process at constant temperature (130 °C) at 1.5 rad s<sup>-1</sup> of rotational speed.

The duration of the rheology data acquisition for pPPDS and pPPGS was set based on PGS initial state, when the already crosslinked sample no longer remained unaltered between the rheometer's plates (≈50 h).

#### 2.3.2. Fourier Transform Infrared Spectroscopy

A Compact FT-IR Spectrometer ALPHA II (Brüker ALPHA-Incom, Spain) was used in attenuated total reflection mode (ATR)

to characterize the chemical composition of monomer mixtures (mPGS, mPPGS, mPPDS), prepolymers (pPGS, pPPGS, pPPDS) and cured PGS in the frequency range 400–4000 cm<sup>-1</sup> at 4 cm<sup>-1</sup> resolution.

## 2.4. Evolution of the HBP Based on Glycerol

### 2.4.1. Fourier Transform Infrared Spectroscopy

FTIR spectroscopy was used as previously described to measure the chemical evolution of PGS synthesis at different time points, from monomeric mixture of SA and Gly (mPGS; 0 h) to the fully cured PGS sample (PGS; 72 h), including different prepolymer time points in between the polymer synthesis (pPGS; 0.5, 1, 2, 3, 4, 8, 12, 16, 20, and 24 h).

### 2.4.2. Titration

A titration method was used to determine the degree of esterification (DE) of the mPGS mixture and its prepolymer (pPGS) as it progressed, up to 24 h, by measuring the free carboxyl groups. For this purpose, an Erlenmeyer flask with 50 mL of a 25:75 wt. % EtOH:THF solution was used to dissolve 100 mg of each sample while stirring. Next, 5 drops of phenol red solution (Sigma Aldrich, Spain) were added as chemical indicator. To perform the titration, a 0.1 M solution of potassium hydroxide (KOH, Sigma-Aldrich, Spain) was added dropwise until the solution color shifted from transparent to pinkish-purple, i.e., when a pH of 7–7.4 was reached. Equation 1 was used to calculate the DE, adapted from<sup>15</sup>:

$$DE = 1 - \frac{(V_1 - V_0)}{V_{\text{mon}} - V_0} \quad (1)$$

where  $V_0$  is the volume of KOH solution used for the blank,  $V_{\text{mon}}$  is the volume used for the mPGS sample, and  $V_1$  is the volume used for each pPGS sample.

### 2.4.3. <sup>1</sup>H-NMR Spectroscopy

<sup>1</sup>H-NMR allowed for assessing the chemical compositions of mPGS and pPGS samples throughout their 24 h progression, as well as determining their reaction degree and branching by means of end-group analysis. Samples were dissolved in Acetone-d<sub>6</sub> (Sigma-Aldrich, Ireland) for this purpose.

The spectra were acquired on a 400 MHz Bruker 400 Varian Inova spectrometer (Varian Medical Systems UK, UK) and samples were reported in parts per million (ppm) relative to the solvent ( $\delta_{\text{H}} = 2.05$  ppm) as an internal reference. Data extracted were analyzed using Mnova Processor software. The area of different proton peaks was calculated in order to determine the amount of pOH and sOH groups reacted with SA carboxyl groups and the DE of mPGS and pPGS samples. Both were obtained according to the adapted equations from Liu, et al.<sup>[33]</sup>

### 2.4.4. Gel Permeation Chromatography

The weight-averaged molecular weight ( $M_w$ ), the number-averaged molecular weight ( $M_n$ ) and polydispersity index (PDI) of the mPGS and pPGS samples were measured by gel permeation chromatography (GPC). A Malvern Omnisec Resolve & Reveal device (Malvern Panalytical, Spain) was used for this purpose, with tetrahydrofuran (THF), 1 mL min<sup>-1</sup>, for the mobile phase, at a temperature of 35 °C by using Malvern Instruments T2000 and T4000 columns. Monodisperse polystyrene was used as standard ( $dn/dc$  0.185).

### 2.4.5. Thermogravimetric Analysis

A thermogravimetric analysis (TGA) was performed in order to simulate a full PGS synthesis containing both steps of polymerization, step 1 from mPGS to pPGS (24 h), and step 2 from pPGS to PGS (48 h). An SDTQ600 thermogravimetric analyzer (TGA, TA Instruments, Spain) was used to register mass loss during a 130 °C isotherm for 72 h at an initial heating ramp rate of 10 °C min<sup>-1</sup> under N<sub>2</sub> flow of 50 mL min<sup>-1</sup>.

### 2.4.6. Differential Scanning Calorimetry

To characterize the thermal properties (melting point temperature) and, indirectly, the trend in the macromer chain growth, differential scanning calorimetry (DSC) measurements of mPGS and pPGS collected up to 24 h were performed in a DSC 8000, double-furnace, power compensation device (Perkin Elmer España SL, Spain). For each experiment, ≈3 mg of sample was weighed on an aluminum pan and sealed. Pans were cooled to -80 °C and scanned up to 60 °C at 20 °C min<sup>-1</sup> under a constant N<sub>2</sub> flow of 50 mL min<sup>-1</sup> while heat flow (W/g) values were measured. The melting point temperature ( $T_m$ ) was determined for each sample from its calorimetric curve.

## 3. Results and Discussion

### 3.1. Effect of the Alcohol Molecular Configuration on Prepolymerisation

Viscosity of monomeric mixtures was monitored at constant temperature of 130 °C for 60 h (Figure 2). The viscosity graph obtained for PGS shows two regions with different slope, while PPDS and PPGS show no changes over time.

From these results, it can be stated that the Gly + SA mixture undergoes a crosslink reaction because of the presence of three hydroxyl groups from Gly. The subtle chemical differences between primary (pOH) and secondary (sOH) hydroxyl do not affect their reactivity when there are only two possibilities. Thus, the differences in their viscosity over time are marginal. The initial linear trend of PGS does not have the same slope as in the other two cases, indicative of ramifications that increase viscosity. The final viscosity increase of PGS is explained because every crosslink that gives rise to the elastomer increases the molecular weight of the macromolecule considerably in a short period

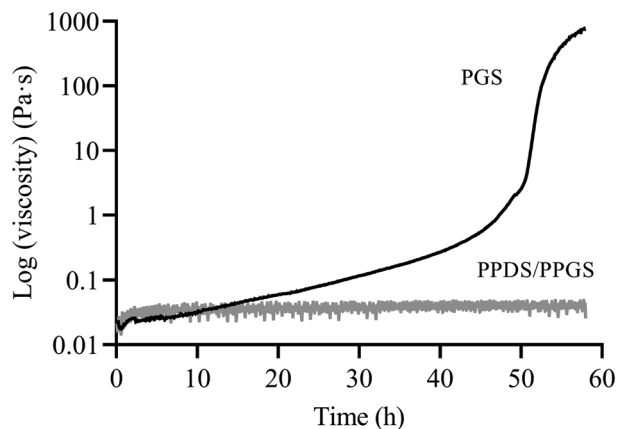


**Figure 2.** Viscosity of mPGS, mPPDS, and mPPGs mixtures over time at 130 °C with PPDS and PPGS represented overlapped.

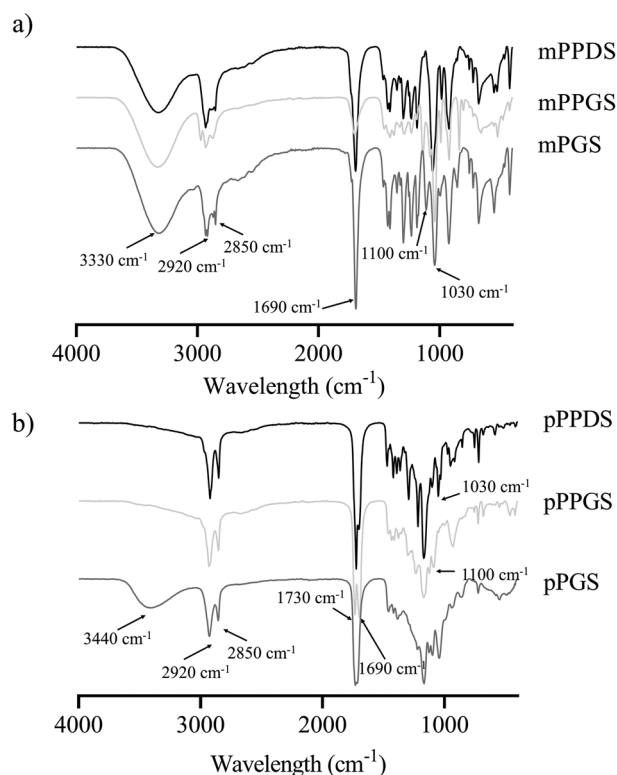


**Figure 3.** FTIR spectra (transmittance, a.u.) of different poly(glycerol sebacate) mixtures prepolymerized under N<sub>2</sub> atmosphere at 130 °C at a) 0 h (m) or b) 24 h (p).

of time. Hence, chain growth is mainly linear at the beginning (first slope) until they quickly assemble (second slope).

Chemical characterization by FTIR allowed for the identification of chemical bonds in monomeric mixtures at the start (m; 0 h) and halfway (p) through the reaction. The obtained FTIR spectra show a broad band at 3300 cm<sup>-1</sup> for hydroxyl groups (O-H stretching) in all samples displayed in **Figure 3**. More precisely, pOH and sOH groups are represented by two sharp peaks at 1030 cm<sup>-1</sup> and 1100 cm<sup>-1</sup>, respectively. Aliphatic C-H absorption appears at 2850–2950 cm<sup>-1</sup> together with the unreacted carboxyl-

related carbonyl (-COOH) at 1700 cm<sup>-1</sup>. After 24 h of reaction, the ester carbonyl (-COO-) peak at 1730 cm<sup>-1</sup> and the C-O peak at 1168 cm<sup>-1</sup> are present in **Figure 3b**.

There is a common trend of the peak for free carboxyl (-COOH) shifting from 1700 cm<sup>-1</sup> to 1730 cm<sup>-1</sup> in correspondence to the reacted ester group (-COO-) in every spectrum over 24 h. The major peak from C-O bonding at 1168 cm<sup>-1</sup> is only present after 24 h.

The spectra of pPPDS present a major signal for COO<sup>-</sup> when compared to free COOH groups, while pPPGS spectra show two peaks with similar intensity at 1700 cm<sup>-1</sup> and 1730 cm<sup>-1</sup>. Finally, the pPGS peak ≈1700–1730 cm<sup>-1</sup> is more homogeneous, presenting both signals together, albeit displaced toward 1730 cm<sup>-1</sup>, which suggests a higher degree of esterification of all the monomeric mixtures because of a higher amount of reacted ester groups than carboxyl.

### 3.2. Does Primary and Secondary Hydroxyl Reactivity of Glycerol Affect PGS Polycondensation?

PGS FTIR spectra from **Figure 4a** present the chemical credential from mPGS (0 h) to pPGS (24 h) and PGS completely cured at 130 °C for 48 h more (total of 72 h). The broad band of maximum intensity of hydroxyl groups is displaced from 3335 cm<sup>-1</sup> in the case of mPGS, to 3438 cm<sup>-1</sup> and 3453 cm<sup>-1</sup> for pPGS and PGS, respectively. The ratio of pOH/sOH represented in **Figure 4b**, taken from pOH and sOH's distinct sharp peaks (1030 cm<sup>-1</sup> and 1100 cm<sup>-1</sup>, respectively), exhibits a decreasing trend in its value, going from ≈2 for mPGS to 0.8 and 0.6 for pPGS and PGS, respectively.

All in all, the results shown indicate that, during the 24 h prepolymerisation, pOH are more likely to react rather than sOH, confirming the linear chain growth of the elastomers.

From <sup>1</sup>H NMR spectra, reacted Gly hydrogen proton signals can be identified between δ3.5–5.5 ppm, including free OH- from unreacted Gly as a broad band ≈δ2.8 ppm. The amount of pOH and sOH groups reacted with SA carboxyl groups were obtained according to the adapted equations from Liu, et al.<sup>[33]</sup> and represented in **Figure 5c**.

The signal for acyl glyceride chemical groups (δ3.5–5.5 ppm), directly related to the progress of the polycondensation reaction, tend to grow from mPGS to pPGS. Based on **Figure 5c**, it can be confirmed that pOH is the first to react by polycondensation, leading to a more linear macromer formulation for pPGS.

### 3.3. Glycerol Influence on the PGS Prepolymerization Reaction Kinetics

Mass loss during PGS synthesis was monitored in a non-confined environment, as represented in **Figure 6a** together with the theoretical boundaries for water mass loss for a 100% conversion (all SA reacts with Gly, H<sub>2</sub>O max), for the Gly excess mass loss from the original equimolar mPGS mixture (H<sub>2</sub>O max + Gly<sub>excess</sub>) and for the case where all Gly gets evaporated, producing no polycondensation at all (Gly<sub>max</sub>). The first slope, at the beginning of the reaction, represents the time of major percentage of weight loss, ≈15% in the first 4 h. The second slope

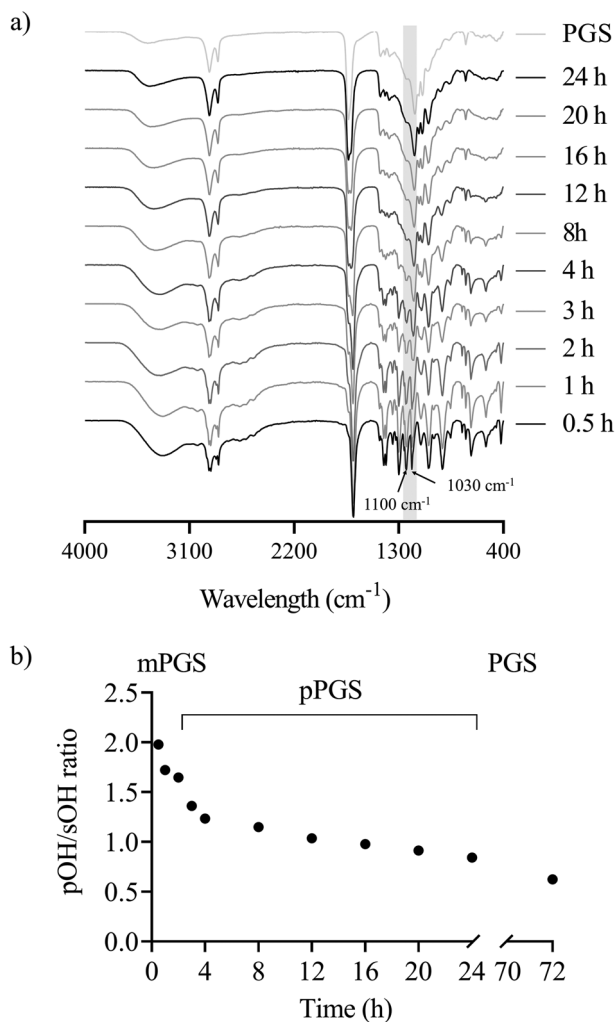


**Figure 4.** a) FTIR spectra (transmittance, a.u.) along PGS synthesis: Step 1, mPGS prepolymerization under N<sub>2</sub> atmosphere conditions at 130 °C from 0 h to 24 h (pPGS). Step 2, curing process at 130 °C for another 48 h until the final polymer is obtained (PGS). b) Ratio between primary hydroxyl groups (pOH) at 1030 cm<sup>-1</sup> and secondary hydroxyl groups (sOH) at 1100 cm<sup>-1</sup> for all the samples from FTIR spectra.

slightly increases while the mass remains stable ≈20% after the first 24 h, with its maximum weight loss at 22% after 72 h.

The continuous flow of N<sub>2</sub> allows for the free evaporation of Gly, which may favor the removal of the resulting water as a by-product. The presence of water alters the kinetic response of the reaction due to the inhibition of the polycondensation reaction.

The final mass loss (22%) is significantly higher than the theoretical mass loss attainable without exceeding the theoretical Gly<sub>excess</sub>, which, assuming a 100% of the reaction among all the functional mPGS groups (-OH and -COOH), is set at ≈23%. Besides water loss, part of the final mass loss can be attributed to the excess of Gly when equimolar ratios were introduced for polymerizing. However, the amount of final mass loss recorded under the thermogravimetric simulation was within the expected hypothetical values of mass loss, highlighting the importance of Gly loss during the synthesis process of PGS. Normalized heat

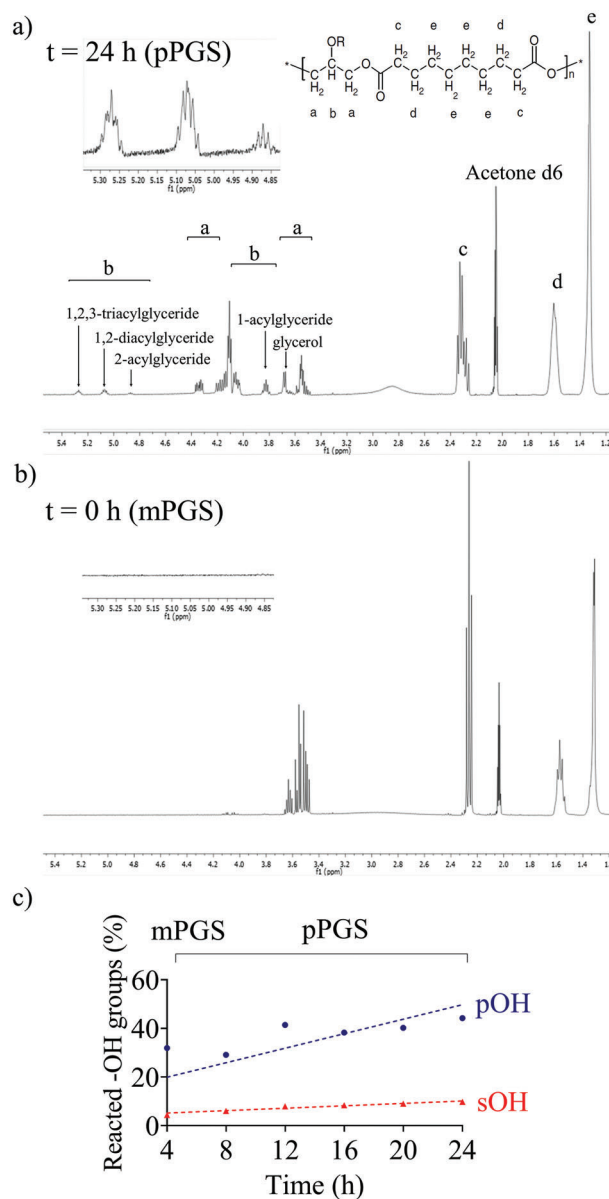


**Figure 5.** <sup>1</sup>H NMR spectrum, in acetone-d<sub>6</sub> (δ<sub>Acetone-d<sub>6</sub></sub> at 2.05 ppm), of a) pPGS (24 h) and b) mPGS (0 h) at 130 °C under N<sub>2</sub>. In the structure are shown the samples chemical assignments. c) Percentage of pOH and sOH groups consumed by polycondensation during the prepolymerization reaction.

power provided to mPGS and pPGS samples were obtained from DSC measurements as shown in Figure 6b. As the synthesis time elapses between mPGS and pPGS, the reaction between oligomers was monitored as they form and grow in the structure of the pPGS. The melting point (T<sub>m</sub>) of pPGS samples exceeds their melting point window range, starting with mPGS highest T<sub>m</sub> at ≈118 °C and down to ≈10 °C for pPGS, repolymerized for 24 h. The only sample that presents a clear glass transition temperature (T<sub>g</sub>) is pPGS after 24 h, slightly under -10 °C.

The oligomers of different sizes can still melt, generating a broad melting window shown in Figure 6b. The presence of a

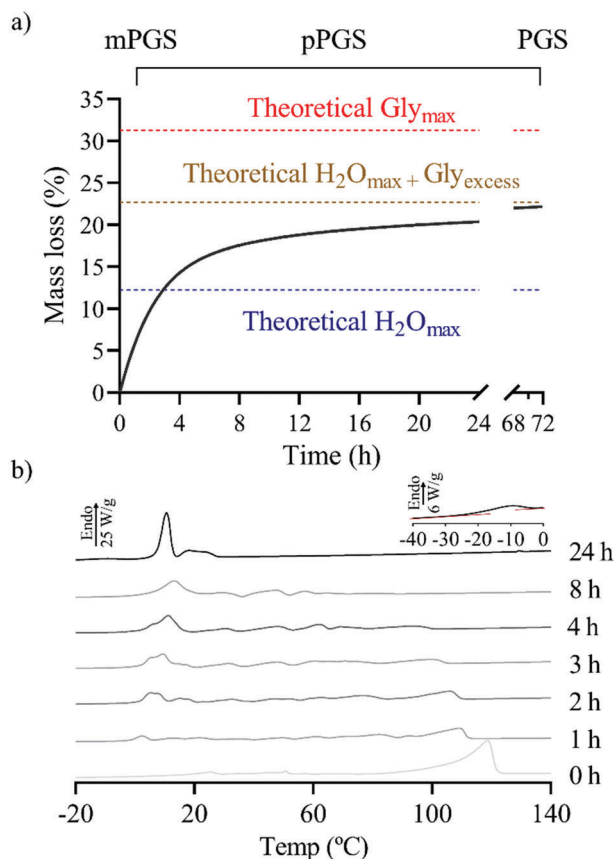


**Figure 6.** a) TGA and b) DSC curves representing the thermal characteristics of PGS pre- and polymerization under  $N_2$  atmospheres for 24 h at  $130\text{ }^\circ\text{C}$ . a) Weight loss (%) versus time (h) is represented. b) The graph presents the temperature ( $^\circ\text{C}$ ) versus normalized heat flow (W/g) of the mPGS at 0 h and the different pPGS samples at different reaction times (1, 2, 3, 4, 8, and 24 h). Inset shows  $T_g$  for 24 h sample.

melting window determines a typical HBP prepolymerization according to bibliography, where the increasing branching has a direct correlation with fewer values of  $T_m$ .<sup>[35]</sup> The pPGS thermal scan presents a more defined  $T_m$  when samples have higher conversion, while lesser prepolymerization in samples is directly related to less homogeneous thermal properties. This thermal profile highlights the heterogeneous kinetic trend of PGS prepolymerization, reducing the mass fraction in the crystalline phase in favor of a more amorphous structure. These results coincide

with previous works in which a homogeneous amorphous HBP is obtained with no melting point and a  $T_g \approx -12\text{ }^\circ\text{C}$ . These properties are expected once the elastomer is fully cured (PGS-72 h).<sup>[20]</sup>

**Figure 7a,b** represents the calculation of the DE by means of titration and  $^1\text{H-NMR}$  values from mPGS and pPGS samples, respectively. For  $^1\text{H-NMR}$  DE calculation, adapted formulas from Liu et al.<sup>[33]</sup> were used. The DE has its maximum value at 80.65% for the titration results and  $\approx 54\%$  for the  $^1\text{H-NMR}$  approximation. This is because, in the second case, the DE is defined based on the proportion of hydroxyl-associated protons. Thus, the maximum degree of esterification of each species cannot reach 100% but stays in lower fractions. However, both samples have their steepest DE increase during the first 4 h of reaction, with similar numerical results,  $\approx 40\%$ . Parallel studies from FTIR spectra were conducted by measuring the ratio of unreacted hydroxyl groups and the ester carbonyl (Figure 7c). The results show a strong downturn of the  $\text{COO}^-/\text{-OH}$  ratio during the same first 4 h of ppolymerization.

From all the data presented in Figure 7 and Figure 6, it can be confirmed that the early stages of polymerization are key factors for the understanding of the PGS, HBP-type synthesis. These first 4 h of the polymerization process are the time when most of the polycondensation process takes place. Linear oligomer chains are obtained that will lead to the first randomly distributed HBP oligomers.

Data extracted from GPC experiments are illustrated in Table 1 presenting a linear trend of number-average molecular weight ( $M_n$ ) and weight-average molecular weight ( $M_w$ ) from  $100\text{ g mol}^{-1}$  at mPGS, to  $\approx 3000\text{ g mol}^{-1}$  with the final pPGS. PDI values are registered at  $\approx 1.5$ , except for mPGS, whose value is higher (PDI = 3.1) due to the Gly and SA individual peak presence.

Shape factors of the molecular weight distribution show chain growth of the PGS has a very regular trend, nearly linear with time. PDI values determine that the polyester behavior is typical for HBP.<sup>[36]</sup>

## 4. Conclusions

This study investigated two major points; how primary and secondary hydroxyls from glycerol are crucial to determine PGS structure and how remarkable effect had the early stages of PGS prepolymerization.

The molecular evolution of this process was monitored over time, thanks to the prepolymerization of the monomeric mixtures of three alcohols (PPD, PPG and Gly). Avoiding Gly loss

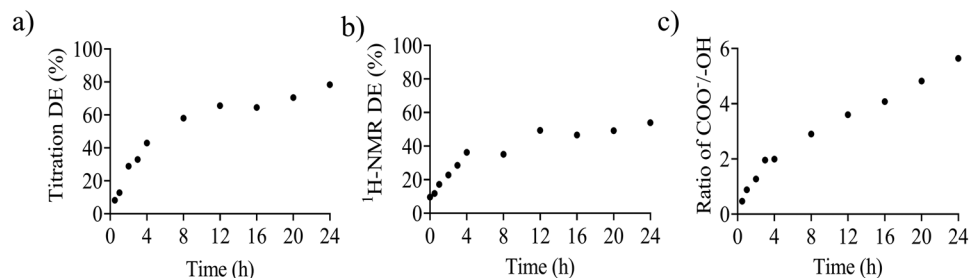


**Figure 7.** DE calculated by means of a) titration and b)  $^1\text{H-NMR}$  of mPGS and pPGS samples, respectively. c) Ratio of  $\text{-OH}/\text{COO}^-$  from FTIR spectra peaks at  $1730\text{ cm}^{-1}$  for  $\text{COO}^-$  groups and the maximum value of  $\text{-OH}$  ranges from  $3300$  to  $3400\text{ cm}^{-1}$ .

**Table 1.** Molecular weights from GPC measurements of mPGS and pPGS samples.  $M_w$ ,  $M_n$ , polydispersity index (PDI) and its ratio evolution from 0 to 24 h.

Time [h]	0	4	8	12	16	20	24
$M_n$ [g/mol]	113.9	757.3	858.9	1464	1580	1906	2204
$M_w$ [g/mol]	355.3	925.4	1224	2190	2118	2717	3510
PDI	3.1	1.2	1.4	1.5	1.3	1.4	1.6

allowed Gly and water by-products to remain into the system. These distinctions confirmed the first of the key synthesis parameters: the chemical hydroxyl distribution defines how the reaction tends to the polycondensation through primary OH rather than secondary OH.

Moreover, most of the polycondensation reaction (DE  $\approx$ 40%) takes place during the first 4 h of the reaction, establishing the polyester backbone structure with a linear and less branched oligomer structure. This explains why synthesis of PGS requires a two-step synthesis to obtain a fully crosslinked PGS HBP.

Afterward, the prepolymer is prone to grow as an HBP once its linear reactivity through primary hydroxyl groups is reduced after 4 h.

Thus, within the first 4 h of the process the polymer grows as numerous low-molecular weight oligomers (typical for a polycondensation reaction), but with propensity to form linear chains instead of the characteristic dendritic expansion of HBPs. This happens spontaneously at the typical, standard synthesis conditions. After this time, since the presence of primary hydroxyls have been reduced significantly, the prepolymerization oligomers tend to condense their chains into branched molecular structures, which eventually will lead to a more crosslinked polymer with elastomeric properties (after 48 h).

In short, we have determined how hydroxyl affinity and the early stages of the PGS HBP synthesis are crucial for the scalability and reproducibility of its final product.

## Acknowledgements

Grant PID2021-128213OB-I00 funded by MCIN/AEI/10.13039/501100011033 and by ERDF A way of making Europe.

## Conflict of Interest

The authors declare no conflict of interest.

## Author Contributions

Conceptualization: RMC, GVF, & AVL; Data curation: RMC, ANP, GVF, & AVL; Formal Analysis: RMC, GVF, & AVL; Funding acquisition: GVF, WW, & AVL; Investigation: RMC, ANP, GVF, WW, & AVL; Methodology: RMC, GVF, WW, & AVL; Project administration: RMC, GVF, AS, WW, & AVL; Resources: RMC, GVF, AS, WW, & AVL; Software: RMC, GVF, AS, WW, & AVL; Supervision: RMC, GVF, AS, WW, & AVL; Validation: RMC, GVF, AS, WW, & AVL; Visualization: RMC, GVF, & AVL; Writing – original draft: RMC, GVF, & AVL; Writing – review & editing: RMC, GVF, AS, WW, & AVL.

## Data Availability Statement

The data that support the findings of this study are available from the corresponding author upon reasonable request.

## Keywords

biomaterials, glycerol, H-NMR, poly(glycerol-sebacate), polymer chemistry

Received: July 29, 2023  
Revised: September 5, 2023  
Published online:

- [1] Y. H. Kim, O. W. Webster, *Macromolecules* **1992**, *25*, 5561.
- [2] C. Gao, D. Yan, *Prog. Polym. Sci.* **2004**, *29*, 183.
- [3] Y. Zheng, S. Li, Z. Weng, C. Gao, *Chem. Soc. Rev.* **2015**, *44*, 4091.
- [4] J. M. J. Fréchet, C. J. Hawker, *React. Funct. Polym.* **1995**, *26*, 127.
- [5] D. Wang, T. Zhao, X. Zhu, D. Yan, W. Wang, *Chem. Soc. Rev.* **2015**, *44*, 4023.
- [6] A. Douka, S. Vouyiouka, L. M. Papaspyridi, C. D. Papaspyrides, *Prog. Polym. Sci.* **2018**, *79*, 1.
- [7] G. Lisak, K. Wagner, P. Wagner, J. E. Barnsley, K. C. Gordon, J. Bobacka, G. G. Wallace, A. Ivaska, D. L. Officer, *Synth. Met.* **2016**, *219*, 101.
- [8] S. Ordanini, F. Cellesi, *Pharmaceutics* **2018**, *10*, 209; .
- [9] Q. Zhu, F. Qiu, B. Zhu, X. Zhu, *RSC Adv.* **2013**, *3*, 2071.
- [10] C. M. Paleos, D. Tsiourvas, Z. Sideratou, L. A. Tziveleka, *Expert Opin. Drug Delivery* **2010**, *7*, 1387.
- [11] A. Jiménez, M. P. G. Armada, J. Losada, C. Villena, B. Alonso, C. M. Casado, *Sens. Actuators, B* **2014**, *190*, 111.
- [12] C. Sun, X. Chen, Q. Han, M. Zhou, C. Mao, Q. Zhu, J. Shen, *Anal. Chim. Acta* **2013**, *776*, 17.
- [13] H. Zhang, L. P. Bré, T. Zhao, Y. Zheng, B. Newland, W. Wang, *Biomaterials* **2014**, *35*, 711.
- [14] R. Rai, M. Tallawi, A. Grigore, A. R. Boccaccini, *Prog. Polym. Sci.* **2012**, *37*, 1051.
- [15] X. Li, A. T. L. Hong, N. Naskar, H.-J. Chung, *Biomacromolecules* **2015**, *16*, 1525.
- [16] X. J. Loh, A. Abdul Karim, C. Owh, *J. Mater. Chem. B* **2015**, *3*, 7641.
- [17] Q. Liu, L. Jiang, R. Shi, L. Zhang, *Prog. Polym. Sci.* **2012**, *37*, 715.
- [18] H. Frey, R. Haag, *Rev. Mol. Biotechnol.* **2002**, *90*, 257.
- [19] Y. Wang, Y. M. Kim, R. Langer, *J. Biomed. Mater. Res.* **2003**, *66A*, 192.
- [20] Á. Conejero-García, H. R. Gimeno, Y. M. Sáez, G. Vilarinho-Feltrre, I. Ortuño-Lizarán, A. Vallés-Lluch, *Eur. Polym. J.* **2017**, *87*, 406.
- [21] M. Nagata, T. Machida, W. Sakai, N. Tsutsumi, *J. Polym. Sci., Part A: Polym. Chem.* **1999**, *37*, 2005.
- [22] Y. Wang, G. A. Ameer, B. J. Sheppard, R. Langer, *Nat. Biotechnol.* **2002**, *20*, 602.
- [23] S. Matsumura, A. R. Hlil, C. Lepiller, J. Gaudet, D. Guay, Z. Shi, S. Holdcroft, A. S. Hay, *J. Polym. Sci., Part A: Polym. Chem.* **2008**, *46*, 3860.
- [24] T. Zhang, B. A. Howell, A. Dumitrascu, S. J. Martin, P. B. Smith, *Polymer* **2014**, *55*, 5065.
- [25] J. M. Kemppainen, S. J. Hollister, *J. Biomed. Mater. Res., Part A* **2010**, *94A*, 9.

- [26] R. Ravichandran, J. R. Venugopal, S. Mukherjee, S. Sundarrajan, S. Ramakrishna, *Tissue Eng., Part A* **2015**, 21, 1288.
- [27] J. Gao, P. M. Crapo, Y. Wang, *Tissue Eng.* **2006**, 12, 917.
- [28] M. Masoudi Rad, S. Nouri Khorasani, L. Ghasemi-Mobarakeh, M. P. Prabhakaran, M. R. Foroughi, M. Kharaziha, N. Saadatkish, S. Ramakrishna, *Mater. Sci. Eng.: C* **2017**, 80, 75.
- [29] A. G. Mitsak, A. M. Dunn, S. J. Hollister, *J. Mech. Behav. Biomed. Mater.* **2012**, 11, 3.
- [30] E. M. Jeffries, R. A. Allen, J. Gao, M. Pesce, Y. Wang, *Acta Biomater.* **2015**, 18, 30.
- [31] Glycerine Producers' Association, in *Chemical Properties and Derivatives of Glycerine*, **1965**.
- [32] Y. Li, W. D. Cook, C. Moorhoff, W. C. Huang, Q. Z. Chen, *Polym. Int.* **2013**, 62, 534.
- [33] Q. Liu, M. Tian, T. Ding, R. Shi, Y. Feng, L. Zhang, D. Chen, W. Tian, *J. Appl. Polym. Sci.* **2007**, 103, 1412.
- [34] V. T. Wyatt, G. D. Strahan, *Polymers* **2012**, 4, 396.
- [35] X. Luo, S. Xie, J. Liu, H. Hu, J. Jiang, W. Huang, H. Gao, D. Zhou, Z. Lü, D. Yan, *Polym. Chem.* **2014**, 5, 1305.
- [36] W. Daniel, S. E. Stiriba, F. Holger, *Acc. Chem. Res.* **2010**, 43, 129.